

SUPERPLASTIC BLOW FORMING OF 2219 ALUMINUM ALLOY

R. Kaibyshev¹, I. Kazakulov¹, D. Gromov¹, D.R. Lesuer² and T.G. Nieh²

¹Institute for Metals Superplasticity Problems, Khalturina 39, Ufa 450001, Russia, rustam@anrb.ru

²Lawrence Livermore National Laboratory, L-342, P.O. Box 808, Livermore, CA 94551, USA,

Keywords: superplasticity, aluminum alloys, blow forming, microstructure evolution

Abstract. Superplasticity in 2219 aluminum alloy was achieved through thermomechanical processing. Tension tests showed that the alloy exhibits superplastic behavior in the temperature range of 450-540°C and strain rates ranging from 2.2×10^{-5} to $1.1 \times 10^{-1} \text{ s}^{-1}$. A maximum elongation-to-failure of 670% was recorded at 500°C and at the initial strain rate of $2.2 \times 10^{-4} \text{ s}^{-1}$. High cavitation level and intensive grain growth were observed. Sheet of the 2219 aluminum alloy was blow formed into conical shape using two different methods: simple negative and backpressure forming. A strain of 2.1 was obtained at 500°C under the backpressure blow forming condition. It was found that elongation to failure under blow forming with backpressure is about 1.5 times higher than that under a simple female forming. Microstructural evolution of blow formed parts was also examined.

Introduction

Superplastic blow forming (SPF) is a viable technique to fabricate complex aluminum alloy sheet parts [1,2]. Superplasticity is observed in materials with a fine grain size, usually less than 10 μm , when the materials are deformed under an appropriate strain rate (typically from 10^{-4} to 10^{-1} s^{-1}) at high temperatures [1,2]. Large superplastic elongation and low flow stress allow the easy forming of complex structural parts, which can not be produced by conventional metal working processes. The use of SPF can sometimes offer a great reduction in manufacturing cost. It is therefore attractive is to make an existing commercial aluminum alloy superplastic through a thermomechanical processing (TMP) which results in the formation of a fully recrystallized structure with ultra fine grain size. It will expand the niche market for SPF of these alloys.

This paper describes different TMPs for achieving superplasticity in the commercial 2219 aluminum alloy. The experimental results provide the optimal superplastic properties of the AA2219, both in tension and in a biaxial test.

Material and Experimental Procedure

The 2219 aluminum alloy with a chemical composition of Al-6.4%Cu-0.3%Mn-0.19%Zr-0.06%Fe (in weight pct.) was manufactured at the Kaiser Aluminum Center for Technology by direct chill casting. The alloy was solution heat treated at 530°C for 6 h. Full details on structural characterization, mechanical tests in tension and the procedure of TMP have been presented previously [3].

A standard cone test in biaxial tension [4] was used to evaluate the superplastic forming capability. The cone angle was ~ 59 deg. Discs with a 120 mm diameter were cut from the as-processed sheets with a thickness of 1.85 mm. These discs were inserted individually into the forming die where they were clamped around their edges so that there was an unrestricted area with a diameter of 100 mm for the forming operation. The die was then heated to a temperature of 500°C and a constant gas pressure was applied. Two ways of constant pressure forming were used:

- (i) forming into a simple female die with a gas pressure ranging from 0.2 to 0.4 MPa;
- (ii) back pressure forming with a net pressure of 0.2 MPa.

In the second case, applied gas pressure on the front and rear sides of the deformed superplastic sheet were 5 and 4.8 MPa, respectively. The forming limit was determined as the fracture strain at which cracking started and sealing broke.

Samples with fixed thickness were sliced from the cone to determine the cavitation level. Metallographic analysis of unetched samples, using the standard point-counting technique, was applied to evaluate cavity size and porosity volume fraction.

Results and Discussion

Mechanical properties in tension. Typical true stress – true strain curves for the thermomechanically-processed 2219 alloy at a fixed strain rate of $2.2 \times 10^{-4} \text{ s}^{-1}$ and different temperatures (450 to 540°C), and at a fixed temperature of 500°C and different strain rates (5.5×10^{-5} to $1.1 \times 10^{-1} \text{ s}^{-1}$) are shown in Figs. 1a and 1b, respectively.

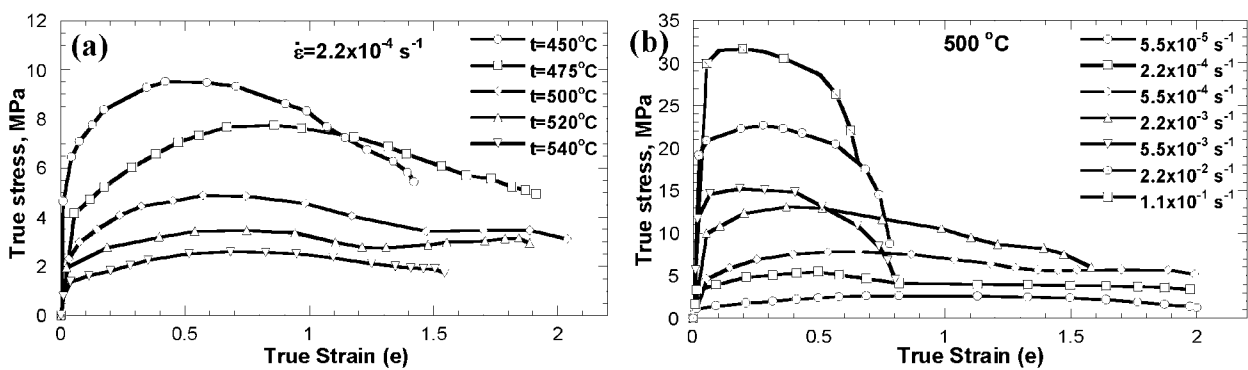


Fig. 1. Tensile true stress – true strain curves of 2219 Al at the different temperatures (a) and at the different strain rates (b).

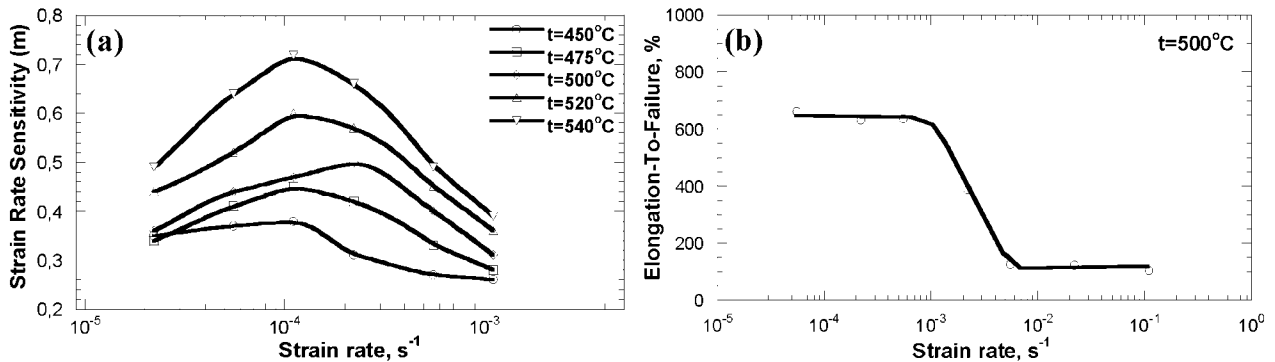


Fig. 2. The variation of strain rate sensitivity as a function of strain rate (a) and elongation-to-failure as a function of strain rate (b).

At all temperatures there is an immediate hardening upon loading, followed by softening. As expected, there is no apparent steady state at low temperatures (for example, at 450°C) or high strain rates (for example, $\dot{\epsilon} \geq 5.5 \times 10^{-3} \text{ s}^{-1}$ at $T = 500^\circ\text{C}$). Apparent steady state exists primarily at high temperatures and low strain rates.

The variation of strain rate sensitivity and elongation-to-failure with strain rate are shown in Figs. 2a and 2b, respectively. The maximum value of strain rate sensitivity occurs in the second region at $\dot{\epsilon} = 2.2 \times 10^{-4} \text{ s}^{-1}$ and tends to decrease on either side of this strain rate (Fig. 2a). The total elongation is about 650% at the strain rate less than about $5 \times 10^{-3} \text{ s}^{-1}$, and decreases rapidly at higher strain rates at $T = 500^\circ\text{C}$ (Fig. 2b).

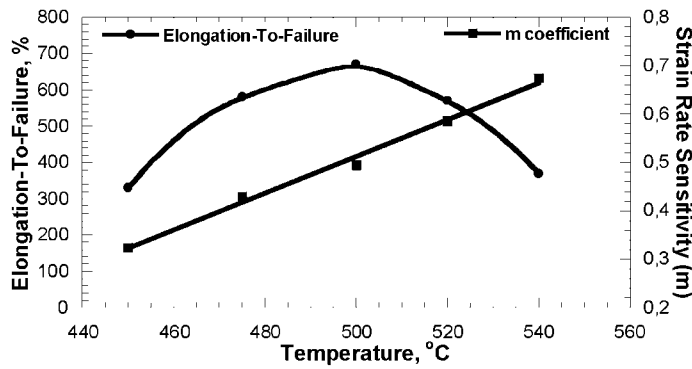


Fig. 3. Elongation-to-failure and strain rate sensitivity as a function of the deformation temperature (at $\dot{\epsilon}=2.2 \times 10^{-4} \text{ s}^{-1}$).

Tensile elongation and strain rate sensitivity as a function of temperature are presented in Fig. 3. The peak elongation occurs at 500°C (at $\dot{\epsilon}=2.2 \times 10^{-4} \text{ s}^{-1}$). The coefficient of strain rate sensitivity m increases in the temperature range of 450-540°C (Fig. 3). In contrast to SUPRAL alloy in which superplasticity takes place at 450°C [5-7], the 2219 alloy exhibits the optimum superplastic properties at a higher temperature of 500°C.

Microstructure after tensile tests. Microstructural evolution of the 2219 alloy was examined under both static annealing (grip section) and dynamic annealing (gauge section) conditions in the temperature range of 450-540°C at a strain rate of $2.2 \times 10^{-4} \text{ s}^{-1}$. Grain sizes observed after static annealing (L_s), dynamic annealing (L_d) and grain aspect ratio (AR) are summarized in Table 1.

Table 1. Grain size in the 2219 alloy after tensile tests at a strain rate of $2.2 \times 10^{-4} \text{ s}^{-1}$.

T, °C	450°C	475°C	500°C	520°C	540°C
L_s (μm)*	12.7/12.9	13.5/14.5	20.3/18.9	20.5/21.5	28.4/26.3
L_d (μm)*	18.5/10.9	19.8/13.0	24.0/16.5	27.1/17.7	31.7/26.8
AR of grains	1.70	1.52	1.45	1.53	1.18

*Numerator and denominator are grain sizes measured in the longitudinal / transverse directions, respectively.

It is readily observed that at $T > 500^\circ\text{C}$ there is significant static grain growth and, in fact, at 540°C the grain size nearly doubles. In the temperature range used in the present study (450-540°C), superplastic deformation causes grain elongated along the tension axis, and the grain aspect ratio decreases with an increase in testing temperature. This is probably associated with the fact that both atom mobility and dislocation glide increase as temperature increases, which enhance grain rotation and accommodation. In fact, grains are virtually equiaxed at $T = 540^\circ\text{C}$.

To evaluate cavitation during superplastic deformation, specimens of the 2219 alloy were deformed up to $e=1.1$ at a strain rate of $2.2 \times 10^{-4} \text{ s}^{-1}$ and different temperatures. Average size of cavities (A), their aspect ratio AR and porosity volume fraction (V) are summarized in Table 2.

Table 2. Cavitation measurements in the 2219 alloy after superplastic deformation.

T, °C	450°C	475°C	500°C	520°C	540°C
A (μm)*	4.2/3.7	5/4.3	5.6/4.6	6.5/6.0	8.9/9.7
AR of cavities	1.13	1.16	1.22	1.08	1.1
V, %	1.4	2.1	3.4	2.2	9.8

*Numerator and denominator are grain sizes measured from the longitudinal / transverse directions, respectively.

Two types of cavities were observed. At $T = 450\text{-}500^\circ\text{C}$, the majority of large cavities were observed to elongate along the tensile direction and had an irregular, jagged shape (Fig. 4a),

suggesting plasticity-controlled cavity growth. Cavity interlinkage was also found in the transverse direction (Fig. 4a) at these temperatures.

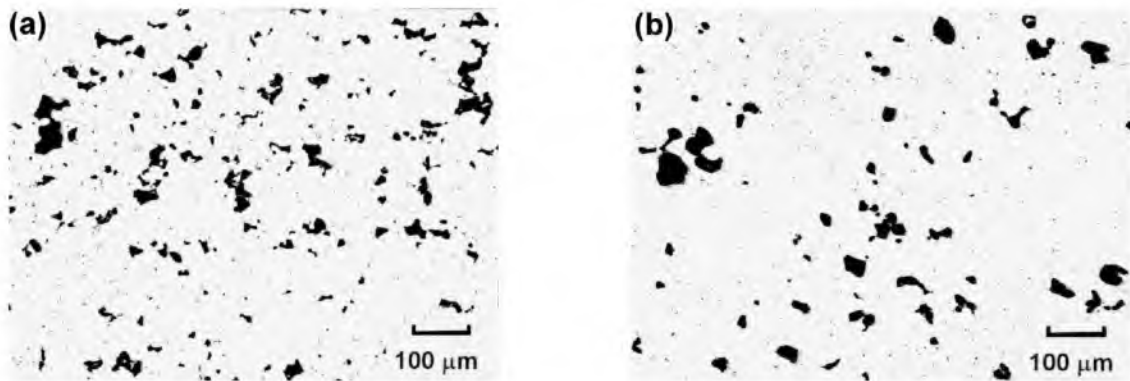


Fig. 4. Microstructures after deformation at $\dot{\epsilon} = 2.2 \times 10^{-4} \text{ s}^{-1}$, $T = 500^\circ\text{C}$, $e=1.1$ (a) and $\dot{\epsilon} = 2.2 \times 10^{-4} \text{ s}^{-1}$, $T = 520^\circ\text{C}$, $e=1.1$ (b)

This type of cavitation is resulted from grain boundary sliding and is dominant at these temperatures. In contrast, small, equiaxed cavities were formed at $T \geq 500^\circ\text{C}$, suggesting an increasing importance of diffusion-controlled cavity growth at high temperatures (Fig. 4b). At high temperatures, fast surface diffusion promotes the formation of small cavities under applied stresses. Meanwhile, plasticity-controlled cavity growth becomes less important with increasing temperature. As a result, a reduction in porosity volume fraction is observed at a higher temperature of 520°C . A dramatic increase in cavity volume at 540°C could be caused by the increasing contribution of extremely fast surface diffusion at this pre-melting temperature.

Superplastic cone forming under biaxial conditions. Discs were subjected to simple female forming (FF) with a gas pressure ranging from 0.2 to 0.4 MPa at $T = 500^\circ\text{C}$ (Fig. 5 a). The sheet material shows poor formability under these conditions. The highest strain in the pole was 1.31 at 0.2 MPa and gradually decreased to 0.97 at 0.4 MPa (Fig. 5 b). Such poor formability is caused by the presence of a high cavitation level during simple superplastic forming. It has been shown [8] that increasing the forming pressure, thus strain rate, results in higher cavitation. Therefore, simple female gas blow forming is probably not suitable for 2219 alloy.

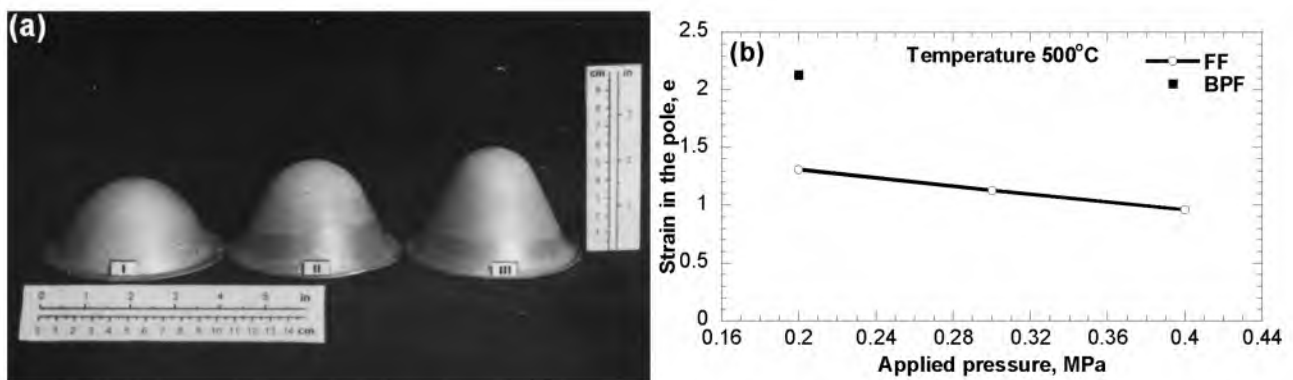


Fig. 5. 2219 Al samples after simple female forming at 500°C . Deformation under different pressures (I - 0.4 MPa; II - 0.3 MPa; III - 0.2 MPa) (a) and the highest strain in the pole as a function of applied pressure for two different forming methods (b).

It is well known [1,8,9] that the use of back-pressure forming (BPF) produces a hydrostatic confining pressure capable of suppressing cavitation. In the present study, it is demonstrated (Fig. 5b) that strain in the pole after BPF at 500°C was 2.1, which is about 1.5 times higher than that after

FF. The forming limit of BPF is generally high within the temperature range where superplasticity occurs.

Microstructure evolution during superplasticity in biaxial test. Grain sizes observed after different types of superplastic forming are shown in Fig. 6. It is seen that superplastic forming produces essentially equiaxed grain. No strain dependence of grain size was found (Fig. 6). At $T=500^{\circ}\text{C}$, the grain size after BPF was found to be higher than that after FF.

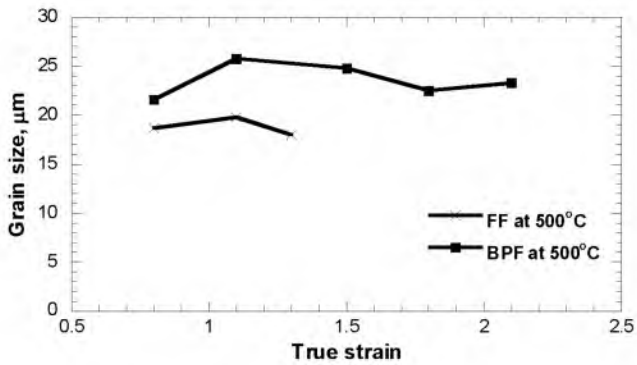


Fig. 6. The effect of gas forming method on grain size at different deformation strains.

Metallographic studies for the AA2219 showed that the feature of cavitation during superplastic FF and BPF is distinctly different. The average cavity size and porosity volume fraction are shown in Fig. 7a and 7b respectively. Angular cavities of large size and voids exhibiting irregular shape were revealed after FF (Fig. 8a). These observations suggest a plasticity-controlled cavity growth mechanism [1], and void coalescence results in pseudo-brittle fracture.

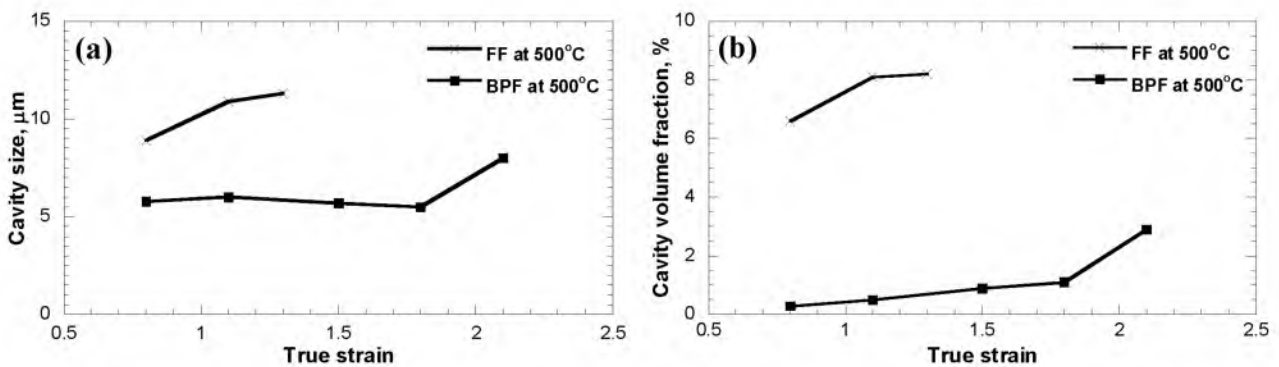


Fig. 7. The effect of gas forming method on cavity average size and volume fraction at different strains.

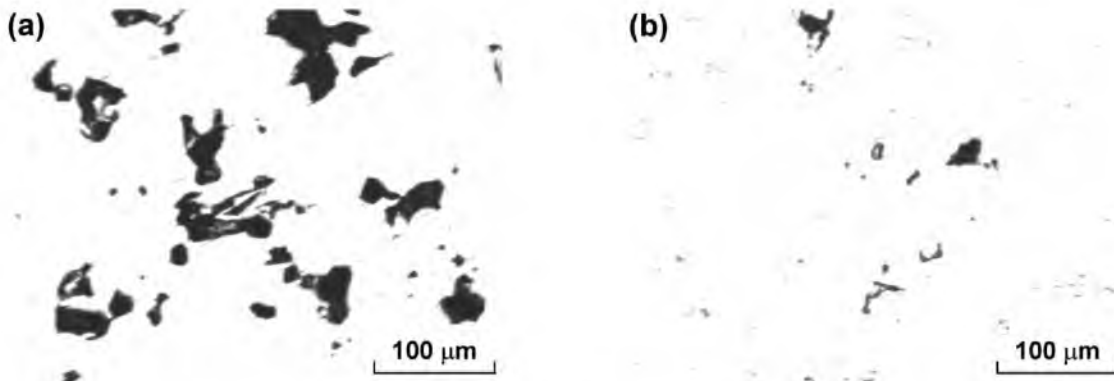


Fig. 8. Cavitation in AA2219 after: (a) simple female forming at 500°C , $e=1.3$; (b) back pressure forming at 500°C , $e=2.1$.

It was reported previously [3] that plasticity-controlled cavity growth took place during superplastic flow in tension and led to specimen failure. It is evident that the maximum forming limit during FF is restricted by extensive cavitation; cavitation damage leads to premature failure of AA2219. Comparing with cavitation data in tension [3] it is concluded that void growth is faster in biaxial test at higher forming rates.

Superimposed back pressure strongly suppresses cavitation (Figs. 7b and 8b) and leads to the preferential formation of fine cavities. These cavities exhibit equiaxed shape suggesting diffusion-controlled growth. An increase in both temperature and strain leads to increasing average cavity size and porosity volume fraction. The fraction of voids with irregular shape and large size tends to grow. However, even at the highest forming limit the volume fraction is still significantly less than ~10%, which is indicative of failure caused by cavity interlinkage [1]. Thus, the superimposition of a confining gas pressure during superplastic forming is effective in restricting cavity growth.

Conclusion

In the present study, we demonstrated that the AA2219 with ultrafine grain structure demonstrates moderate superplastic characteristics in tension test and superior superplastic properties in biaxial test under superimposed back pressure. Specifically,

1. It was shown that the 2219 aluminum alloy with an initial grain size of 12 μm exhibits superplasticity. The maximum elongation-to-failure of 670% was recorded at $T = 500^\circ\text{C}$ and at a strain rate of $2.2 \times 10^{-4} \text{ s}^{-1}$.
2. The 2219 aluminum alloy demonstrates a marginal forming limit during female forming ($e=1.31$) and superior ductility ($e=2.1$) under superimposed back pressure forming.
3. The application of back pressure suppresses cavitation during gas blow forming.

References

- [1] J. Pilling, N. Ridley: *Superplasticity in crystalline solids* (The Institute of Metals, London 1989).
- [2] T.G. Nieh, J. Wadsworth, and O.D. Sherby: *Superplasticity in metals and ceramics*, (Cambridge University Press, Cambridge, UK, 1997).
- [3] R. Kaibyshev, I. Kazakulov, D. Gromov, F. Musin, D.R. Lesuer and T.G. Nieh: *Scr. Mater.* Vol. 44 (2001), p. 2411.
- [4] R.J. Lederich, S.M.L. Sastry, M. Hayase and T.L. Mackay: *J. Metals* Vol. 8 (1982), p. 16.
- [5] R. Grimes, M.J. Stowell and B.M. Watts: *Metals. Tech.* Vol. 3 (1976), p. 154.
- [6] B.M. Watts, M.J. Stowell, B.L. Baikie and D.G.E. Owen: *Met. Sci.* Vol. 10 (1976), p. 189.
- [7] R.H. Bricknell and J.W. Edington: *Metall. Trans.* Vol. 10A (1979), p. 1257.
- [8] M.G. Zelin, S. Guillard and P.K. Chaudhury: *Mater. Sci. Forum* Vol. 243-245 (1997), p. 137.
- [9] A.J. Barnes: *Mater. Sci. Forum* Vol. 170-172 (1994), p. 701.